

Article

Fuzzy Adaptive Energy Management Strategy for a Hybrid Agricultural Tractor Equipped with HMCVT

Zhen Zhu ¹, Lingxin Zeng ¹, Long Chen ¹, Rong Zou ² and Yingfeng Cai ^{1,*}¹ Automotive Engineering Research Institute, Jiangsu University, Zhenjiang 212013, China² School of Mechanical Engineering, Jiangsu University, Zhenjiang 212013, China

* Correspondence: caicaixiao0304@126.com

Abstract: In order to solve the problem of high fuel consumption and poor emission performance in high horsepower tractors, a parallel hybrid tractor system was designed using a dual power source of an engine and motor matched with a hydro-mechanical continuously variable transmission (HMCVT). An equivalent fuel consumption minimization strategy (ECMS) was used for power distribution of this hybrid system. To address the problem of poor adaptability of the equivalence factor to different working cycles in the conventional ECMS, a fuzzy adaptive equivalent fuel consumption minimization strategy (FA-ECMS) was proposed. A fuzzy PI controller based on battery SOC (State of Charge) feedback was designed to adjust the equivalence factor in real time, so as to achieve adaptive control of the equivalence factor. The physical model of the system was built by SimulationX, and the model of the control strategy was built using Matlab/Simulink. Two typical cycles of tractor plowing and road transportation were simulated. Under ECMS, the fuel consumption of the hybrid agricultural tractor was 14.3 L and 1.19 L in one plowing cycle and one transport cycle, respectively, with final battery SOC values of 60.75% and 60.32%, respectively. Under FA-ECMS, the hybrid farm tractor consumed 13.34 L and 1.13 L in one plowing cycle and one transport cycle, respectively, with final battery SOC values of 60.27% and 60.17%, respectively. The results showed that, with the introduction of a fuzzy PI controller to dynamically adjust the equivalence factor, the overall fuel consumption was reduced by 6.71% and 5.04%, respectively, and the battery power maintenance performance was improved. The designed control strategy could achieve a more reasonable power distribution between the engine and motor while maintaining the balance of the battery SOC.

Keywords: hybrid agricultural tractor; hydro-mechanical continuously variable transmission; fuzzy adaptive; equivalent fuel consumption minimization strategy; energy saving



Citation: Zhu, Z.; Zeng, L.; Chen, L.; Zou, R.; Cai, Y. Fuzzy Adaptive Energy Management Strategy for a Hybrid Agricultural Tractor Equipped with HMCVT. *Agriculture* **2022**, *12*, 1986. <https://doi.org/10.3390/agriculture12121986>

Academic Editor: Massimo Cecchini

Received: 29 October 2022

Accepted: 21 November 2022

Published: 23 November 2022

Publisher's Note: MDPI stays neutral with regard to jurisdictional claims in published maps and institutional affiliations.



Copyright: © 2022 by the authors. Licensee MDPI, Basel, Switzerland. This article is an open access article distributed under the terms and conditions of the Creative Commons Attribution (CC BY) license (<https://creativecommons.org/licenses/by/4.0/>).

1. Introduction

China's "14th Five-Year Plan" proposes to vigorously develop agricultural machinery and enhance the core competitiveness of agricultural machinery. Tractors are a typical representative of agricultural power machinery and play an important role in agricultural production activities. According to statistics released by China's Ministry of Agriculture and Rural Affairs, the number of tractors in China had exceeded 20 million by 2021 [1]. However, in the past 10 years, the annual production of tractors has shown a declining trend year by year, which is due to changes in the market demand for tractors. People tend to look for alternative agricultural equipment because the power requirements for tractor operation are overwhelming. This has led to a sharp decline in the production of small and medium horsepower tractors, which accounted for a high proportion of the original number, and large horsepower tractors now dominate [2,3]. Traditional tractors have many shortcomings, such as poor driving experience, high fuel consumption, and poor emission performance [4,5]. With the advancements of the electrification of agricultural machinery, researchers have conducted studies on pure electric and hybrid tractors [6,7]. Limited by battery capacity and output power, pure electric tractors are generally used in small and

medium horsepower tractors. For large horsepower tractors working in large farms, hybrid electric tractors are the better choice [8,9]. For hybrid tractors, formulating effective energy management strategies is the key to improving fuel economy and reducing emissions [10].

The principle of energy management of hybrid electric tractors is to calculate the optimal power distribution among different power sources under the given power demand, so as to achieve the goal of fuel saving and consumption reduction at the end of the corresponding driving cycle [11]. Recently, there have been studies on energy management strategies for hybrid vehicles [12–14], and the applications are relatively mature. However, the special operating environment and work requirements of tractors are very different from those of other vehicles, such as automobiles that are transported on structured roads. Tractors have two main working cycles: the operating cycle and the road transport cycle. Depending on the different agricultural machinery and tools being carried, the operating cycles can be further divided into seeding, plowing, rototilling, harvesting, and other cycles, and the load is variable during the process of operation [15]. Relevant studies have shown that the use ratio of a tractor in the speed range of 4 km/h~20 km/h accounts for more than 80% of the whole life cycle, so the engine works in the low-speed and high-power ranges most of the time, resulting in a relatively low overall efficiency [16]. In terms of an energy management strategy, due to the non-plug-in hybrid tractor's on-board electrical system, energy is limited; however, the tractor has a high-power demand most of the time, so the engine is in the start state in most cases. Generally, this will not cause the engine's frequent start-stop phenomenon to appear and the motor mainly plays an assistance role [17].

The application of rule-based energy management strategies in hybrid tractors is relatively mature. Xu Li-you et al. designed an energy management strategy based on fuzzy rules for hybrid tractors equipped with fuel cells and batteries, and the effectiveness of the strategy was verified by simulation [18]. However, the formulation of fuzzy rules depends on the experience of the designer. Chao Jia et al. compared the effects of thermostat-based and power-following control strategies on the fuel consumption and emission performance of series hybrid agricultural tractors under different cycles, showing that the power-following control strategy had better fuel economy, but was prone to produce more particulate emissions [19]. The rule-based control strategies mentioned above are easy to apply, but it is difficult to achieve optimal control because of their strong subjectivity. Dynamic programming (DP) is a global optimization method, which decomposes a large problem into several small problems and then recursively solves them to obtain the global optimal solution [20]. For dual-motor-driven electric tractors, Li Tong-hui et al. proposed a real-time adaptive energy management strategy by integrating the advantages of the stochastic dynamic programming (SDP) global optimization algorithm and the extreme value search instantaneous optimization method. The results show that this strategy has real-time performance and can improve the working mileage of the tractor [21]. Li Yin-ping et al. used a dynamic programming algorithm to optimize the electric tractor with a supercapacitor and battery composite, and summarized a rule-based control strategy, which effectively reduced power consumption [22]. Although dynamic programming can achieve optimal control, it needs to predict cycle conditions in advance, and has a large amount of calculations, so it is not suitable for real-time applications.

The equivalent consumption minimization strategy (ECMS) is a representative of the instantaneous optimization strategy. Based on Pontryagin's minimum principle (PMP), this strategy converts battery power consumption to engine fuel consumption by introducing the concept of "oil-electric equivalent factor", and calculates the instantaneous optimal torque distribution combination with the goal of minimizing instantaneous total fuel consumption. This strategy has a moderate amount of computation and is suitable for real-time application to tractors [23]. However, the equivalent factor has the problem of poor working cycle adaptability, which has a great impact on the electric power maintenance type of hybrid tractor. Researchers have proposed a variety of adaptive strategies for equivalent factors [24,25]. Limited by the working environment and working state of the tractor, adaptive strategies based on driving cycle prediction and driving pattern recognition are

rarely applied to the tractor. The equivalent factor is usually adjusted by feedback from the battery SOC. The PI controller was used in [26] to adjust the equivalent factor in real time, which is a simple and effective method that can be applied in real time. However, it does not consider the impact of the proportional and integral coefficient setting on the robustness of the ECMS strategy.

In this study, for the hybrid tractor equipped with HMCVT, first, rules are set based on the universal characteristic curve of the engine and battery SOC to achieve operating mode division. Then, with the goal of minimizing equivalent fuel consumption, fuzzy rules are introduced to adjust the proportional and integral coefficients of the PI controller to improve the robustness of the system. A fuzzy adaptive model of the equivalent factor based on SOC feedback was established to achieve real-time accurate correction of the equivalence factor. Finally, the effectiveness of the control strategy is verified by simulation.

The rest of the paper is presented as follows. The configuration and specifications of the hybrid tractor powertrain system are illustrated in Section 2, while the mathematical model of the main components of the powertrain system is presented in Section 3. Then, Section 4 introduces the overall control strategy framework of the hybrid tractor and establishes the FA-ECMS energy management strategy for power distribution. Comparative simulation studies are conducted and analyzed in Section 5. Section 6 concludes the paper.

2. System Structure of Hybrid Tractor

2.1. System Architecture

The hybrid tractor powertrain system configuration studied in this paper is depicted in Figure 1, and the main system component parameters are depicted in Table 1. The system consists of the engine, battery, motor/generator, hydro-mechanically continuously variable transmission (HMCVT), coupler, final drive, differential, wheel side reducer, power-take-off (PTO), and some other components. By controlling the engagement and separation of the relevant clutch and brake components, five modes can be provided: pure engine drive mode, pure electric drive mode, hybrid drive mode, driving charging mode, and regenerative braking mode.

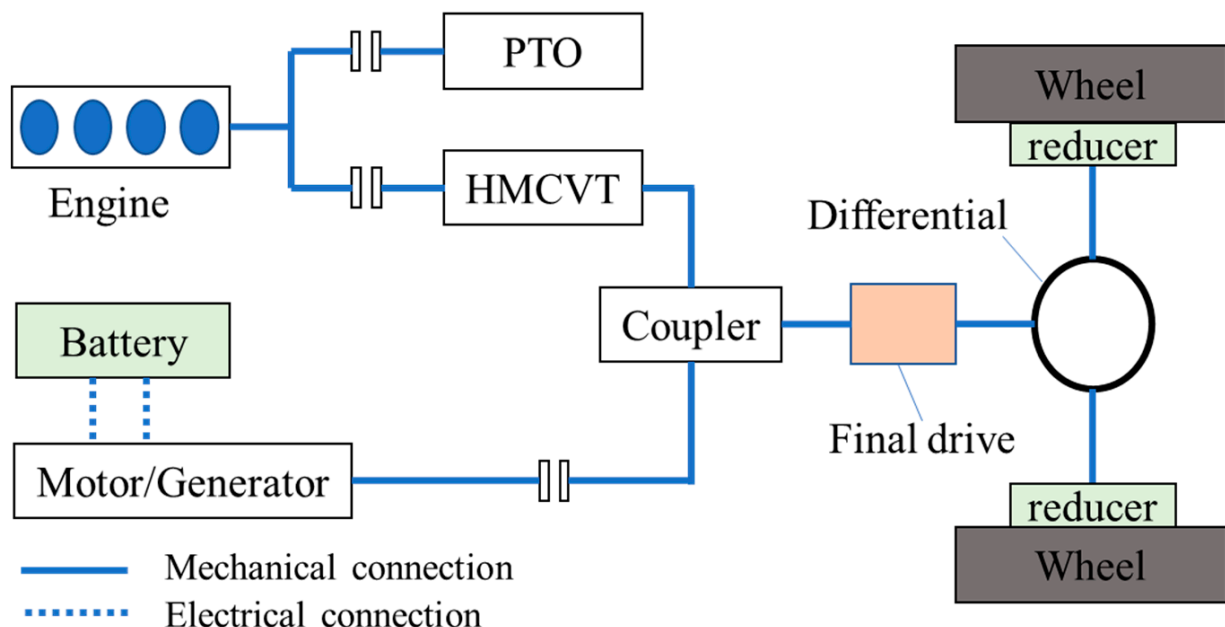


Figure 1. System configuration of hybrid tractor.

Table 1. Parameters of main components of the powertrain.

Items	Parameters	Value
Tractor	Tractor mass	8260 kg
	Drive wheel radius	0.875 m
Engine	Rated power	132 kW
	Rated speed	2300 rpm
	Maximum torque	750 N·m
	Minimum fuel consumption rate	203 g/(kW·h)
Motor	Maximum/rated power	85/45 kW
	Maximum/rated torque	130/250 N·m
Battery	Rated capacity	45 A·h
	Rated voltage	360 V
Driveline	HMCVT ratio	1.0~3.57
	Final drive ratio	3.7
	Wheelside reduction ratio	6.4

2.2. Transmission Mode of HMCVT

Unlike the hybrid tractor with a multi-speed mechanical stepped transmission, the parallel hybrid tractor studied in this paper is equipped with a hydro-mechanical CVT that combines the high efficiency of the mechanical transmission with the high torque of the hydraulic transmission. The transmission structure principle is shown in Figure 2. The mechanical part consists of a planetary gear mechanism and fixed ratio gear, and the hydraulic part includes a variable pump and quantitative motor and related hydraulic components. The power flow from the engine passes through the diversion or convergence of the planetary gear and fixed ratio gear, and is finally output from the output port of the gearbox.

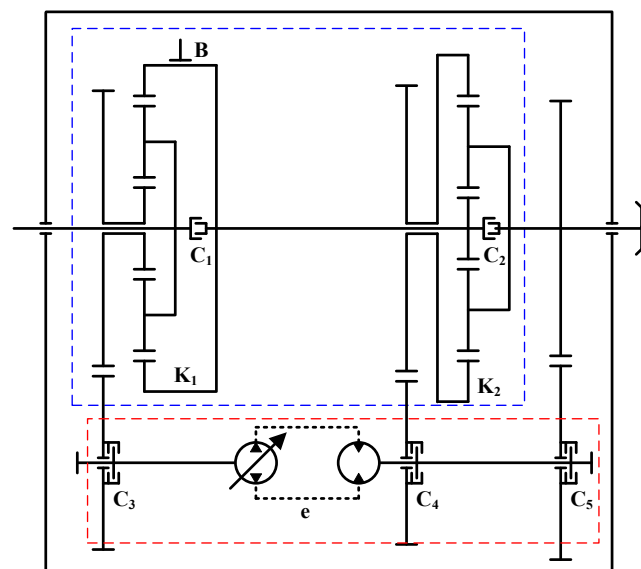


Figure 2. Structural schematic diagram of hydraulic-mechanical continuously variable transmission. Note: B is the brake; C1~C5 refers to clutch 1~5; K1 and K2 are the characteristic parameters of planetary gear.

Table 2 shows the speed ratio characteristics of the hydro-mechanical CVT. By selectively engaging the relevant clutch and brake components and adjusting the displacement ratio of the variable pump in the hydraulic transmission structure, stepless speed regulation between gears of the transmission can be achieved, thus providing hydraulic gear (H), mechanical gear (M), and hydraulic mechanical gear (HM). The relationship equation be-

tween the speed ratio and displacement ratio shown in Table 2 leads to the speed regulation characteristic curve of HMCVT shown in Figure 3. The speed regulation characteristic curve reflects the trend of the transmission speed ratio with the change of the variable pump displacement ratio. The transmission efficiency of the hydraulic gear is low, but this gear can transmit larger torque and is mainly applied when the tractor starts. When the tractor is in road transport or field work cycles, it mainly uses the mechanical hydraulic gear. The stepless speed regulation in the segment between each gear is articulated through synchronous switching between gears and gears in order to realize the entire stepless speed regulation of the transmission device.

Table 2. Speed ratio characteristics of HMCVT.

Gears	Brake and Clutch Engagement Status						Speed Ratio i_g
	C1	C2	C3	C4	C5	B	
F(H)	▲	—	▲	—	▲	—	$\frac{i_5 i_7}{i_6}$
R(H)	—	—	▲	▲	—	▲	$\frac{(1+k_2)i_5 i_6}{(1+k_1)k_2 e}$
F(M)	▲	▲	—	—	—	—	1
F(HM1)	—	▲	▲	▲	—	—	$\frac{i_5 i_6 + k_1 e}{(1+k_1)e}$
F(HM2)	▲	—	▲	▲	—	—	$\frac{i_5 i_6 (1+k_2)}{i_5 i_6 + k_2 e}$

Note: F represents forward gear; R represents reverse gear; H is hydraulic gear; M is mechanical gear; HM is hydraulic mechanical gear; i is speed ratio; k is planetary gear characteristic parameter; e is displacement ratio of variable pump, the range is $[-1,1]$; “▲” and “—” represent component engagement and separation, respectively.

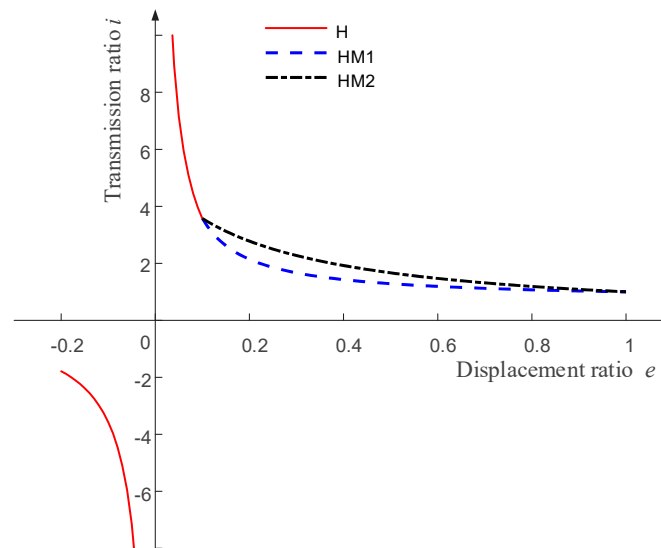


Figure 3. Speed regulation characteristic curve of hydraulic-mechanical continuously variable transmission.

3. System Modeling

3.1. Engine Model

Tractors are usually equipped with diesel engines. The steady-state model of the engine is established by the test data. The surface of engine-specific fuel consumption versus engine speed and torque was constructed by interpolating the data, as shown in Figure 4. Therefore, the mathematical model of engine fuel consumption can be expressed as follows:

$$Q = \frac{1}{3.6 \times 10^9 \times \rho} \int_0^t T_e \omega_e b_e dt \tag{1}$$

where Q is engine fuel consumption (L); T_e is the engine output torque (N·m); ω_e is the angular speed of the engine ($\text{rad}\cdot\text{s}^{-1}$); b_e is specific fuel consumption rate ($\text{g}\cdot\text{kWh}^{-1}$); ρ is the density of diesel fuel ($\text{g}\cdot\text{mL}^{-1}$); t is time (s).

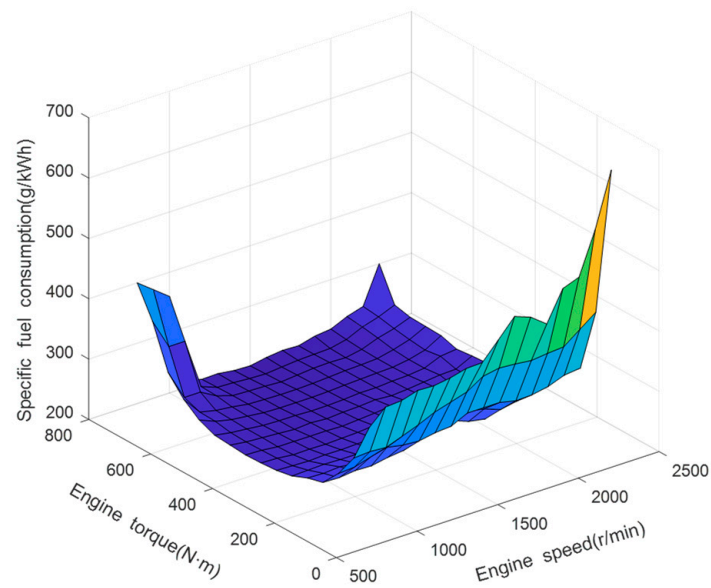


Figure 4. Engine fuel consumption surface.

3.2. Motor Model

The efficiency model of the motor is constructed by data interpolation, as shown in Figure 5. The motor can operate in an electric mode or power generation mode, and its power can be expressed as:

$$P_m = T_m \omega_m \eta_m^{-\text{sgn}(T_m)} / 1000 \tag{2}$$

where T_m is the output torque of the motor (N·m); ω_m is the angular speed of the motor ($\text{rad}\cdot\text{s}^{-1}$); P_m is motor power (kW); η_m is the motor efficiency, when $T_m > 0$, it represents motor efficiency, and when $T_m < 0$, it represents generator efficiency.

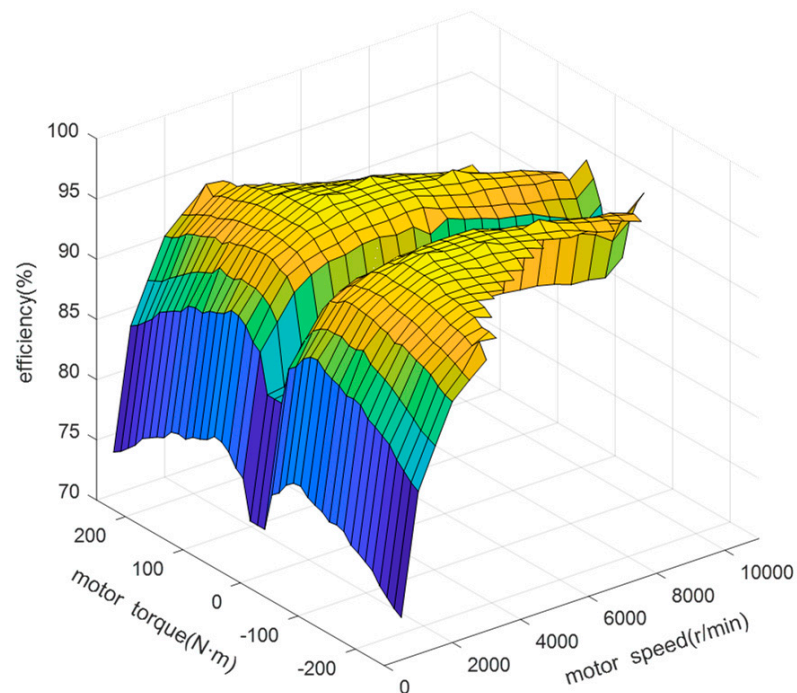


Figure 5. Efficiency characteristics of motor in electric/generation mode.

3.3. Battery Model

The battery model uses the Rint model, which equates the battery to an ideal voltage source U_{oc} and a resistor R in series. This model is used to study the dynamic response of the battery when carrying a load and is applicable to the study of energy management in hybrid vehicles. It can be described by the following equation:

$$\frac{dSOC}{dt} = \frac{U_{oc} - \sqrt{U_{oc}^2 - 4P_{bat}R_{bat}}}{2R_{bat}Q_{bat}} \tag{3}$$

$$P_{bat} = -\frac{dSOC}{dt}U_{oc}Q_{bat} \tag{4}$$

In Equations (3) and (4), U_{oc} is the open-circuit voltage of the battery(V); P_{bat} is battery output power (W); R_{bat} is the equivalent internal resistance of the battery (Ω); Q_{bat} is the rated capacity of the battery (A·h).

The curves of battery charge/discharge internal resistance and voltage variation with battery charge are shown in Figure 6.

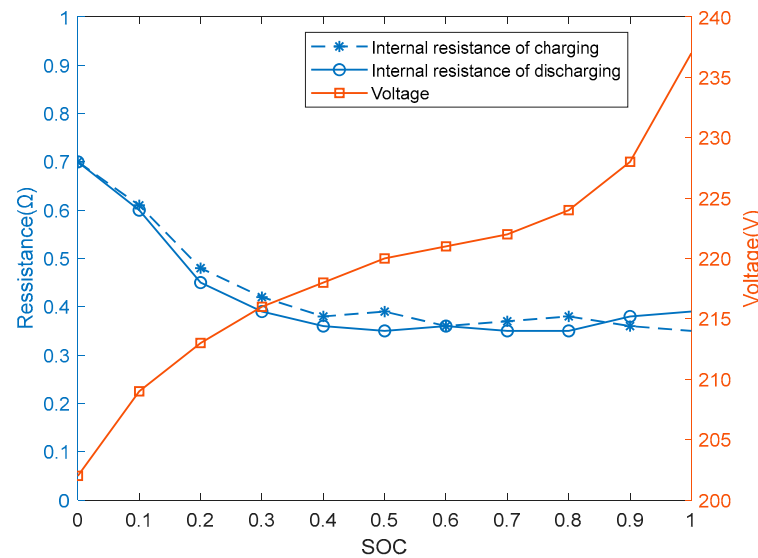


Figure 6. Battery charge and discharge characteristic curve.

3.4. Transmission Model

For the hydro-mechanical continuously variable transmission studied in this paper, it is necessary to match the corresponding speed ratio when the engine is working. Taking economy as the control target, by fitting the data of the throttle opening and engine economic speed, the calculation formula of the best economic speed of the tractor under different throttle openings is obtained as shown in Equation (5). Equation (6) shows the relationship between the engine speed and the driving speed of the whole machine. The economic speed ratio control map of the hydro-mechanical continuously variable transmission is obtained by combining Equations (5) and (6), as shown in Figure 7.

$$n_{e_opt} = -210\alpha^4 - 150\alpha^3 + 810\alpha^2 + 1000\alpha + 750 \tag{5}$$

$$v_a = 0.377 \frac{n_e r_w}{i_g i_o i_w (1 + \delta)} \tag{6}$$

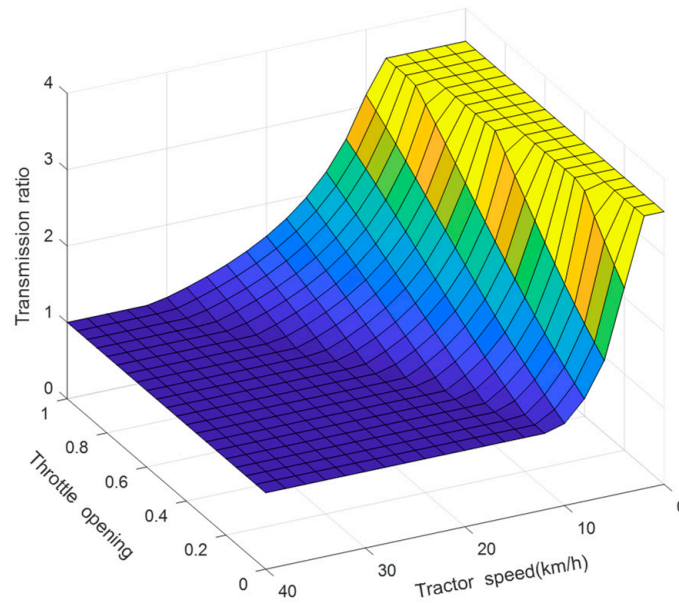


Figure 7. Economic speed ratio surface of hydro-mechanical continuously variable transmission.

In Equations (5) and (6), α is the throttle opening; n_{e_opt} is the engine optimum economy speed (rpm); n_e is the engine speed (rpm); v_a is the actual tractor speed ($\text{km}\cdot\text{h}^{-1}$); r is the tractor drive wheel radius (m); i_g is the transmission ratio, i_o is the main reducer ratio, i_w is the wheelside reducer ratio; δ is the drive wheel slip rate.

3.5. Longitudinal Dynamics Model of the Tractor

The built simulation model is mainly used to verify the vehicle energy management related control strategy, so only the longitudinal dynamics model of the tractor is considered, expressed by Equation (7).

$$\begin{cases} T_t i_g i_o i_w \eta_t - T_w = J_w \dot{\omega}_w \\ T_w = (F_T + \frac{1}{2} \rho C_D A v_a^2 + m g f \cos \theta + m g \sin \theta) r_w \\ v_a = \omega_w r_w / (1 + \delta) = \omega_{in} r_w / i_g i_o (1 + \delta) \end{cases} \quad (7)$$

where T_t is the driving torque (N·m); i_g is the transmission ratio, i_o is the drive axle ratio, i_w is the wheelside reduction ratio; T_w is the driving wheel torque (N·m); J_w is the equivalent rotational inertia of the driving wheel ($\text{kg}\cdot\text{m}^2$); ω_w is the angular speed of the driving wheel ($\text{rad}\cdot\text{s}^{-1}$); F_T is the hook traction force (N); ρ is the air density ($\text{kg}\cdot\text{m}^3$); C_D is the air drag coefficient, A is the windward area (m^2); m is the mass of the tractor (kg); v_a is the actual speed of the tractor ($\text{m}\cdot\text{s}^{-1}$); g is the acceleration of gravity ($\text{m}\cdot\text{s}^{-2}$); θ is the slope ($^\circ$); δ is the slip rate of the driving wheel; ω_{in} is the angular speed of the transmission input ($\text{rad}\cdot\text{s}^{-1}$); r_w is the radius of the driving wheel (m).

4. Real-Time Optimized Energy Management Strategy

4.1. Control Strategy Framework

In order to improve the fuel economy of the high horsepower hybrid tractor in road transportation and field operation cycles, for the parallel hybrid tractor equipped with hydro-mechanical CVT studied in this paper, an equivalent fuel consumption minimization energy management strategy based on equivalent factor fuzzy adaptive is proposed, as shown in Figure 8.

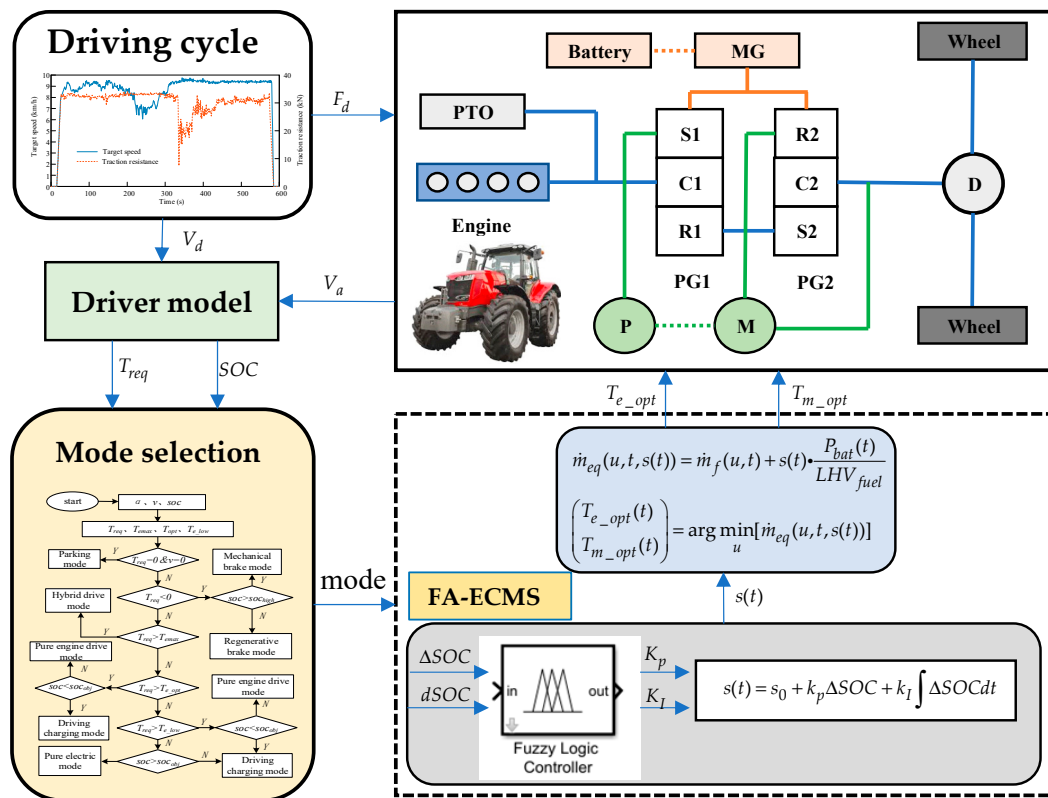


Figure 8. Energy management control strategy framework of the hybrid tractor.

First, the driver model controls the acceleration or brake pedal opening α according to the difference between the target vehicle speed V_d and the actual vehicle speed V_a . The demand torque T_{req} is calculated from the pedal opening α obtained from the driver model and the actual speed V_a from the feedback of the tractor. Then, based on the optimization curve of the engine, the efficient working area of the engine is divided, and the corresponding logic threshold is set to divide the working mode of the hybrid tractor. In braking mode, the output braking torque is T_b . In pure engine drive mode and pure electric drive mode, the demand torque is provided by a single power source. In hybrid drive mode and driving charging mode, the torque is allocated by fuzzy adaptive equivalent fuel consumption minimum strategy (FA-ECMS). The equivalent factor $s(t)$ is adjusted in real time by PI controller, and the fuzzy rules are introduced to optimize the proportional and integration coefficients of the PI controller, so as to obtain the real-time energy management strategy of hybrid tractor which can be applied online.

4.2. Mode Division Based on Logical Thresholds

An ECMS control strategy considering mode switching has been proposed in the literature [27]. By calculating the equivalent fuel consumption corresponding to each operating point in all selectable modes, a particle swarm algorithm is used to search for the operating point with the lowest equivalent fuel consumption, and the operating mode and torque distribution corresponding to this optimal operating point is used as the output, thus achieving the integration of operating mode switching and torque distribution. However, this method tends to lead to frequent switching of operating modes and is relatively computationally intensive. For this reason, this paper adopts a more mature and simple method, which is based on the engine optimized operating curve to divide the engine torque interval, as shown in Figure 9, where T_{e_max} is the maximum engine torque, T_{e_opt} is the engine economically optimal torque curve, and T_{e_low} is the minimum torque in the engine efficiency interval.

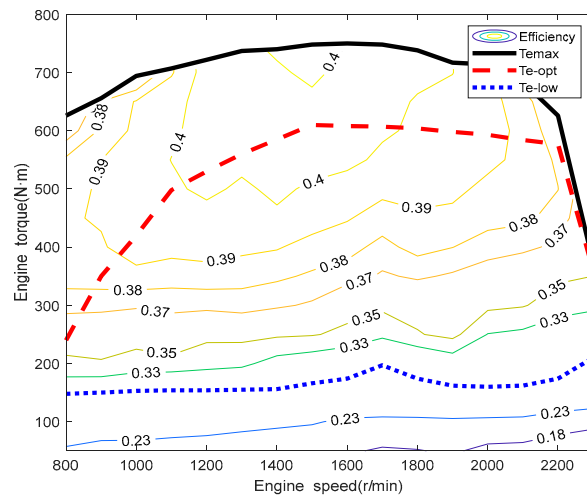


Figure 9. Division of engine torque interval.

Based on the optimal operating curve of the engine, the operating mode division rules are developed as shown in Figure 10. Firstly, the demand torque T_{req} is calculated from the tractor speed v and pedal opening α , and the maximum torque T_{e_max} , the optimal torque T_{e_opt} , and the efficient interval torque threshold T_{e_low} of the engine at the current speed are obtained from the engine universal characteristic curve. The overcharge and overdischarge of the battery have a great impact on their working performance and service life. Therefore, the battery maintenance target value SOC_{obj} is set as 0.6, and the highest and lowest fluctuation ranges, SOC_h and SOC_l , are set as 0.8 and 0.4, respectively. Combining the demand torque T_{req} and the battery SOC signal, the logic threshold is set to judge the working mode during driving. Finally, the working mode division rules of the parallel hybrid tractor are obtained.

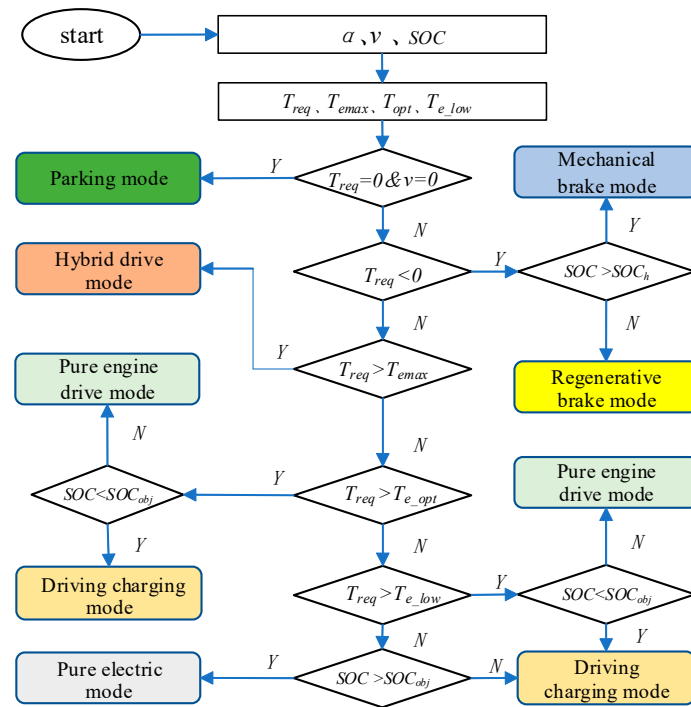


Figure 10. Flow chart of mode division.

4.3. Fuzzy Adaptive Equivalent Fuel Consumption Minimization Strategy

For the hybrid tractor studied in this paper, the battery cannot be actively charged through the external power grid, so it needs to consume fuel to maintain a stable battery

SOC at the end of the working cycle. In a given operating cycle, the power consumed by the battery will be replenished in the subsequent driving and operation process through the driving charging mode or regenerative braking mode, and the final power consumption is actually converted to fuel consumption. For this reason, it is necessary to formulate an appropriate power source torque distribution strategy to reduce fuel consumption as much as possible, while maintaining the balance of battery SOC.

The main idea of the equivalent fuel consumption minimization strategy (ECMS) is to equate the electric consumption of the hybrid vehicle to the fuel consumption by introducing an oil-electric equivalence factor, followed by the equivalent total fuel consumption as a unified indicator for optimal control [28]. The sum of engine fuel consumption and battery equivalent fuel consumption under each instant is minimized as the objective function, and the optimal solution is found under the condition that the relevant constraints are satisfied. The mathematical model is as follows:

$$\begin{cases} \dot{m}_{eq} = \dot{m}_f + \dot{m}_{bat} \\ \dot{m}_{bat} = s(t) \cdot \frac{P_{bat}(t)}{LHV_{fuel}} \end{cases} \quad (8)$$

where \dot{m}_{eq} is the instantaneous equivalent total fuel consumption, \dot{m}_f is the instantaneous engine fuel consumption, \dot{m}_{bat} is the instantaneous equivalent fuel consumption of the battery, P_{bat} is the battery output power, $s(t)$ is the oil-electric equivalence factor, LHV_{fuel} is the low heating value of fuel.

Taking the minimum total fuel consumption of the tractor in the time domain $[t_0, t_f]$ as the control objective, the system objective function J is defined as:

$$J = \int_{t_0}^{t_f} \dot{m}_{eq}(x(t), u(t), t) dt \quad (9)$$

where the state variable $x(t)$ is defined as the battery SOC value and the control variable $u(t)$ is the torque distributed between the engine and motor at each moment.

$$\dot{x}(t) = \dot{SOC}(t) = \frac{-\eta_{bat} \cdot I_{bat}}{Q_{bat}} \quad (10)$$

$$u(t) = \begin{pmatrix} T_{e_d}(t) \\ T_{m_d}(t) \end{pmatrix} \quad (11)$$

where $\dot{SOC}(t)$ is the battery charge or discharge change rate, η_{bat} is the battery charge or discharge efficiency, I_{bat} is the current, and Q_{bat} is the rated capacity of the battery.

The objective function should meet the following constraints:

$$\begin{cases} T_{e_min} \leq T_e \leq T_{e_max} \\ \omega_{e_min} \leq \omega_e \leq \omega_{e_max} \\ T_{m_min} \leq T_m \leq T_{m_max} \\ \omega_{m_min} \leq \omega_m \leq \omega_{m_max} \\ SOC_l \leq SOC \leq SOC_h \end{cases} \quad (12)$$

where T_{e_max} and T_{e_min} are the upper and lower limits of engine torque, respectively; ω_{e_max} and ω_{e_min} are the upper and lower limits of engine speed, respectively; T_{m_max} and T_{m_min} are the upper and lower limits of motor torque, respectively; ω_{m_max} and ω_{m_min} are the upper and lower limits of motor speed, respectively; and SOC_h and SOC_l are the upper and lower limits of battery SOC, respectively; where $SOC_l = 0.4$ and $SOC_h = 0.8$.

According to the Pontryagin principle of minimal values, the instantaneous Hamiltonian function is constructed as:

$$H\{u, t, \lambda(t)\} = \dot{m}_f(x, u, t) + \lambda(t) \cdot \dot{x}(u, t) \quad (13)$$

where H is the Hamiltonian function and λ is the Lagrangian operator, the optimal sequence of control variables that minimizes the Hamiltonian function can be expressed as:

$$u^{opt}(t) = \underset{u}{\operatorname{argmin}}[H(u, t, \lambda(t))] \tag{14}$$

By taking Equations (4) and (10) into Equation (13), we can obtain:

$$H\{u, t, \lambda(t)\} = \dot{m}_f - \lambda(t) \frac{LHV_{fuel}P_{bat}}{U_{oc}Q_{bat}} \tag{15}$$

Combine Equation (8) with Equation (15) to define the oil-electric equivalence factor.

$$s(t) = - \frac{\lambda(t)LHV_{fuel}}{Q_{bat}U_{oc}(t)} \tag{16}$$

When the set oil-electric equivalent factor is small, the equivalent fuel consumption of the battery is relatively low, and the energy management system tends to use electricity, which can easily lead to overdischarge of battery SOC. On the contrary, when the equivalent factor is large, the energy management system is more inclined to use oil, resulting in the rise of battery SOC deviating from the target value. In order to improve the fuel economy of the tractor and maintain the stability of battery SOC, it is necessary to adjust the oil-electric equivalence factor online. In this paper, the equivalence factor is corrected in real time by introducing a PI controller, and the mathematical model of the equivalence factor can be expressed as:

$$s(t) = s_0 + K_p\Delta SOC + K_I \int \Delta SOC dt \tag{17}$$

$$\Delta SOC = SOC_{ref} - SOC(t) \tag{18}$$

where s_0 is the initial equivalent factor, SOC_{ref} is the reference SOC, $SOC(t)$ is the actual SOC, K_p is the proportionality coefficient, and K_I is the integration coefficient.

The setting of the proportional coefficient K_p and the integral coefficient K_I also has an impact on the value of the equivalent factor. In order to improve the robustness of the system, an optimization model of the equivalent factor based on fuzzy control is established, and a fuzzy controller is introduced to modify the proportional and integral coefficient. A two-dimensional fuzzy controller is set. The deviation ΔSOC and the deviation change rate $dSOC$ between the SOC reference value and the actual value are taken as inputs of the fuzzy inference system, and the correction amounts ΔK_p and ΔK_I of the proportional coefficient K_p and the integral coefficient K_I are taken as outputs. The final values of K_p and K_I can be expressed by the following equation:

$$K_p = K_{p0} + \Delta K_p \tag{19}$$

$$K_I = K_{I0} + \Delta K_I \tag{20}$$

Define “positive large (PB)”, “positive small (PS)”, “zero (ZR)”, “negative small (NS)”, and “negative large (NB)” as five linguistic variables to describe the variation of ΔSOC , $dSOC$, ΔK_p , and ΔK_I . Using the triangular function as the affiliation function, the theoretical domain of the input quantity is set to $[-0.1, 0.1]$, and the theoretical domains of the output quantities ΔK_p and ΔK_I are set to $[-6, 6]$ and $[-1, 1]$, respectively. The membership functions of the input and output quantities are shown in Figure 11.

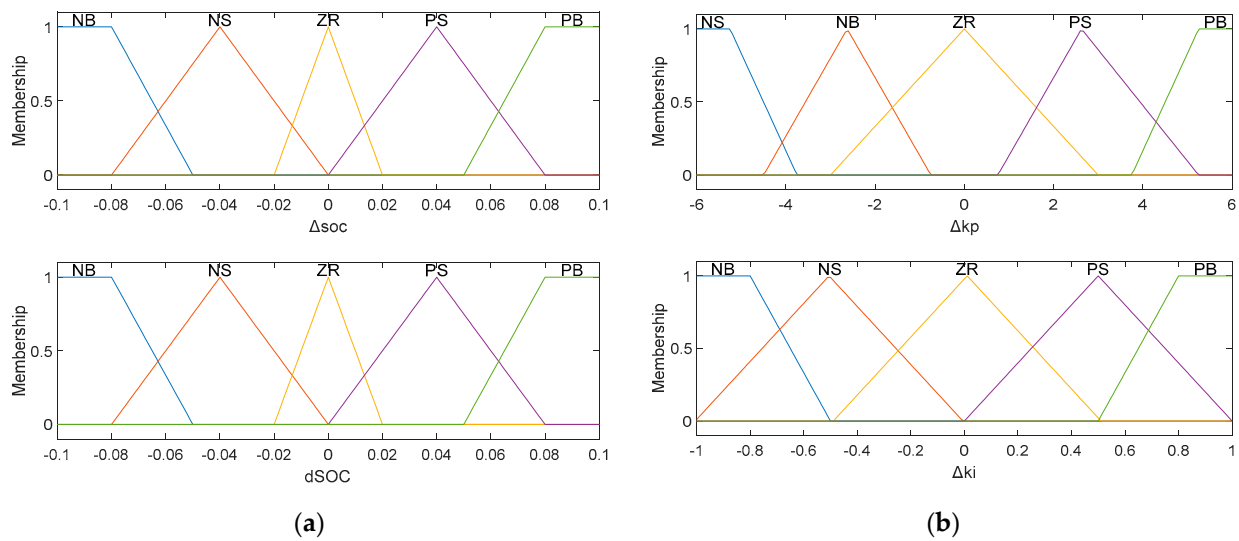


Figure 11. (a) Membership functions of input variables; (b) membership functions of output variables.

When $\Delta SOC > 0$, the actual battery power is less than the reference battery power, at which time the proportional coefficient K_P and the integral coefficient K_I are proportional to the equivalent factor. Depending on the magnitude of the power deviation ΔSOC and the deviation change rate $dSOC$, K_P and K_I are corrected to increase the equivalent factor, so that the energy management system tends to directly slow power consumption or charge. Similarly, when $\Delta SOC < 0$, the power consumption trend can be adjusted by modifying the coefficient. Based on this, the fuzzy rules shown in Tables 3 and 4 are developed for the proportional coefficient correction ΔK_P and the integral coefficient correction ΔK_I , respectively, achieving a more accurate adjustment of the equivalent factor.

Table 3. Control rules of ΔK_P .

		ΔSOC				
		NB	NS	ZR	PS	PB
$dSOC$	NB	PB	PS	PS	PS	ZR
	NS	PS	PS	PS	ZR	ZR
	ZR	PS	PS	ZR	NS	NS
	PS	PS	ZR	NS	NS	NS
	PB	ZR	NS	NS	NB	NB

Table 4. Control rules of ΔK_I .

		ΔSOC				
		NB	NS	ZR	PS	PB
$dSOC$	NB	NB	NB	NB	NS	ZR
	NS	NB	NS	NS	ZR	ZR
	ZR	NS	NS	ZR	PS	PS
	PS	NS	ZR	PS	PS	PS
	PB	ZR	PS	PB	PB	PB

The fuzzy rule surfaces of the correction quantities ΔK_P and ΔK_I are shown in Figure 12. The equivalent factor is further adjusted by the correction of the proportional and integral coefficients, so as to construct a fuzzy adaptive model of the equivalence factor based on the battery SOC feedback.

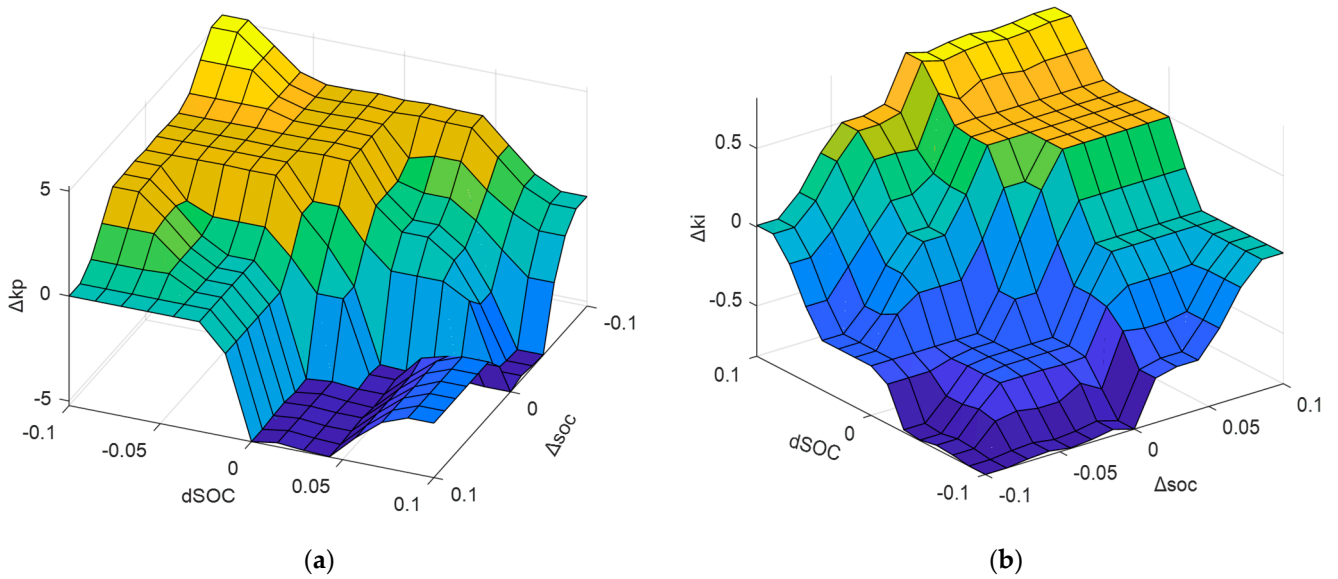


Figure 12. (a) Fuzzy regular surface of output ΔK_p ; (b) fuzzy regular surface of output ΔK_i .

5. Simulation Analysis

5.1. Simulation Model Construction

The physical model of the hybrid tractor was built by ITI SimulationX, as shown in Figure 13. The control strategy model was built on Matlab/Simulink, and the .dll file was generated by the compiler for SimulationX to realize the joint simulation. In order to verify the effectiveness of the proposed ECMS with fuzzy adaptive adjustment of the equivalent factor, it was compared with the conventional ECMS with fixed equivalent factor.

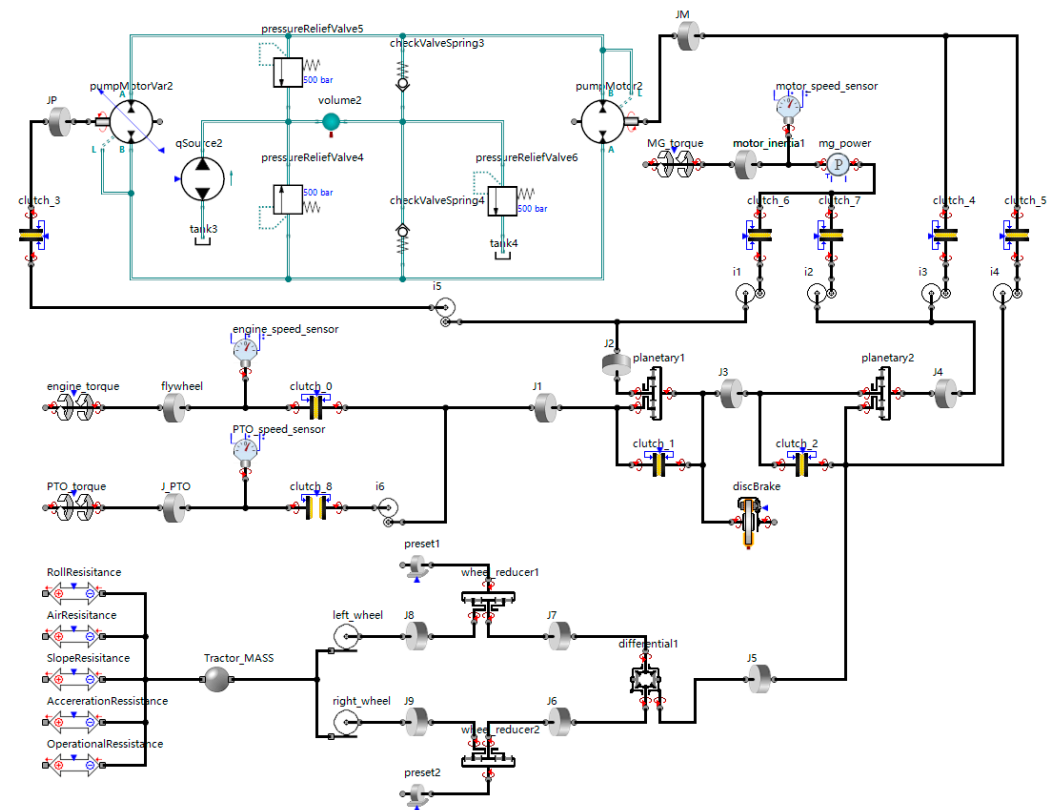


Figure 13. Physical model of tractor based on SimulationX.

5.2. Cycle Construction

The working cycles of hybrid tractors can be divided into road transport cycles and field operation cycles. Field operations can be divided into sowing, plowing, rotary plowing, harvesting, and other working cycles according to the different agricultural machinery and tools equipped, and whether the power-take-off (PTO) works [29]. According to the size of the load received by the tractor during operation, it can be divided into light load, medium load, and heavy load operating cycles. In operation working cycles, tractors usually maintain a stable driving speed to pull agricultural machinery and tools in order to work.

According to the working cycle data of agricultural tractors published by the U.S. Environmental Protection Agency (EPA), the plowing working cycle of the hybrid tractor studied in this paper is established [30]. As shown in Figure 14, the plowing cycle lasts for 600 s, in which the average traction resistance is 36.60 kN and the average operating speed is 8.86 km/h. Since there is no standard road transport working cycle for tractors, considering that tractors often operate in the suburbs and the driving speed is generally not more than 40 km/h, the road transport working cycle of tractors is constructed with reference to the low-speed EUDC cycle, as shown in Figure 15. The working cycle duration is 400 s, the maximum speed is 30.01 km/h, and the average speed is 19.84 km/h.

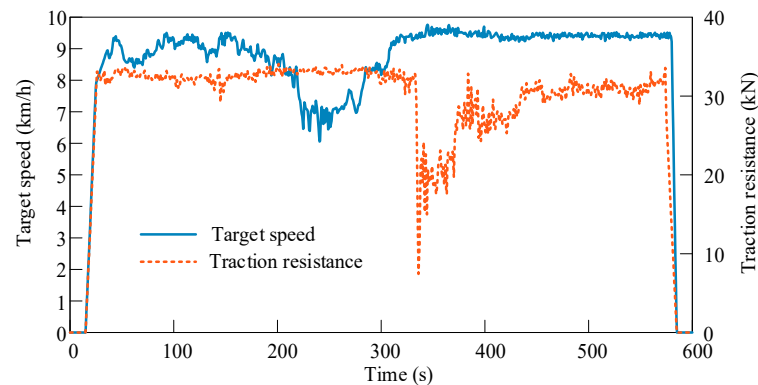


Figure 14. Plowing cycle.

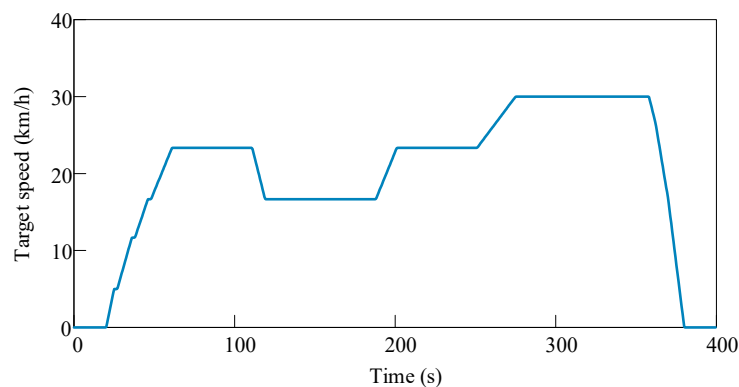


Figure 15. Road transport cycle.

5.3. Analysis of the Plowing Cycle

The tractor speed tracking under the plowing cycle is shown in Figure 16a,b. From the figure, it can be seen that the speed of the tractor is better under the FA-ECMS strategy. The average error between the target speed and the actual speed is 0.0003 km/h. The actual speed and the target speed greatly deviate at about 335 s, and the maximum deviation is 1.13 km/h. This is because the traction resistance has a large mutation at about 335 s, which is caused by the model response delay. The whole simulation model is still reliable. Figure 16c,d shows the power distribution between the engine and the motor under the

traditional ECMS strategy and the FA-ECMS strategy proposed in this paper, respectively, under the plowing cycle. The plowing cycle is a heavy-duty operation cycle with high power demand, and the engine provides the main part of the power demanded by the whole machine, while the motor plays the function of auxiliary operation. Combined with the change of battery SOC trajectory in Figure 16e, it can be seen that FA-ECMS strategy makes more use of the motor, and the charging and discharging power of the motor greatly fluctuates compared with the ECMS strategy, and has better power maintenance performance. The final SOC values under ECMS strategy and FA-ECMS strategy are 60.75% and 60.27%, respectively. Figure 16f shows the comparison of fuel consumption under the two strategies. Fuel consumption under the traditional ECMS strategy and the FA-ECMS strategy is 14.30 L and 13.34 L, respectively. After the fuzzy adaptive adjustment of the equivalent factor, the fuel consumption of the tractor is reduced by 6.71%. It can be seen in Figure 17 that the engine operating points based on FA-ECMS strategy are more distributed in the low fuel consumption area of the engine universal characteristic map, and the load rate of the engine is increased.

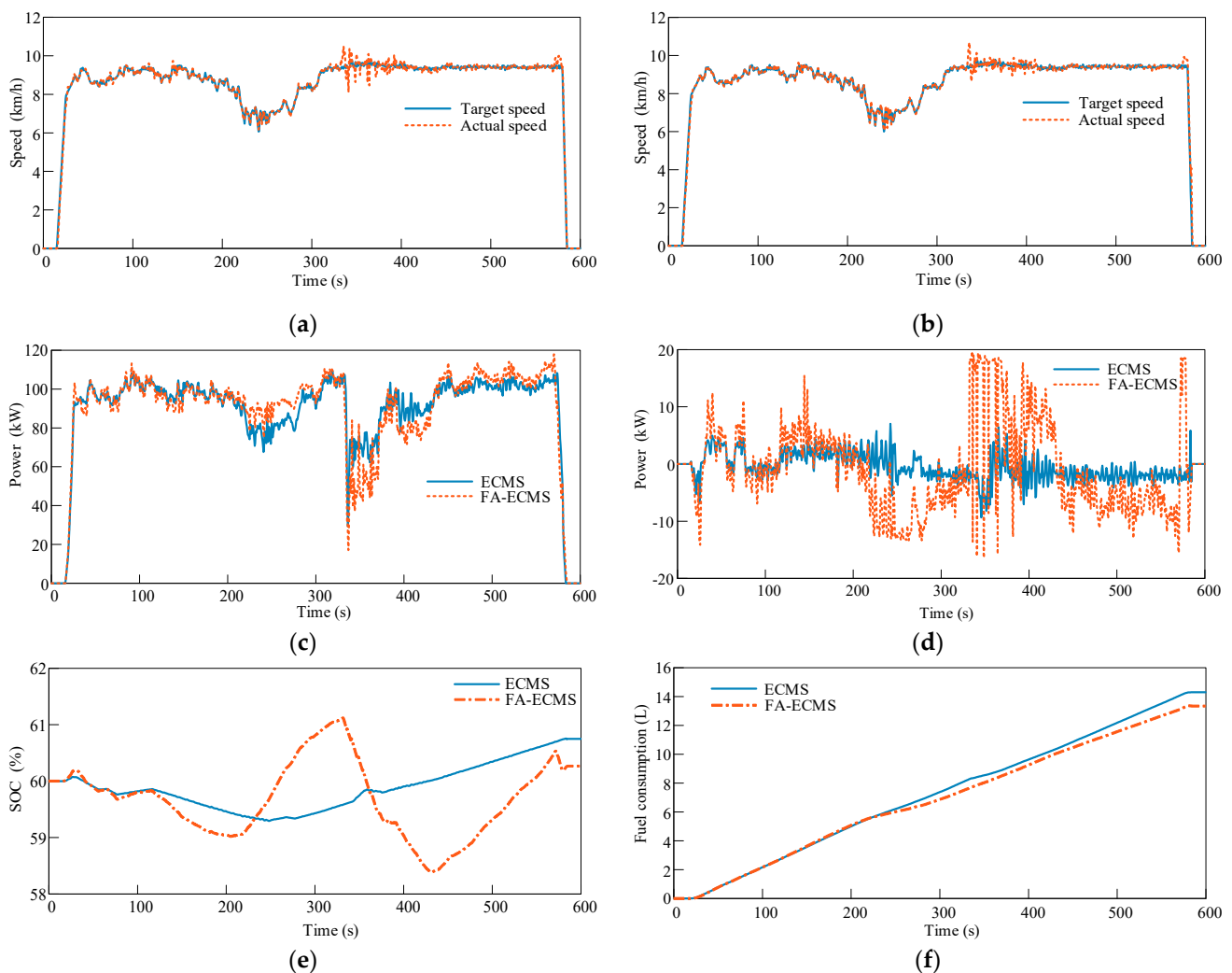


Figure 16. Results of plowing cycle: (a) speed following situation under ECMS; (b) speed following situation under FA-ECMS; (c) engine power comparison; (d) motor power comparison; (e) comparison of battery SOC trajectories; (f) comparison of fuel economy.

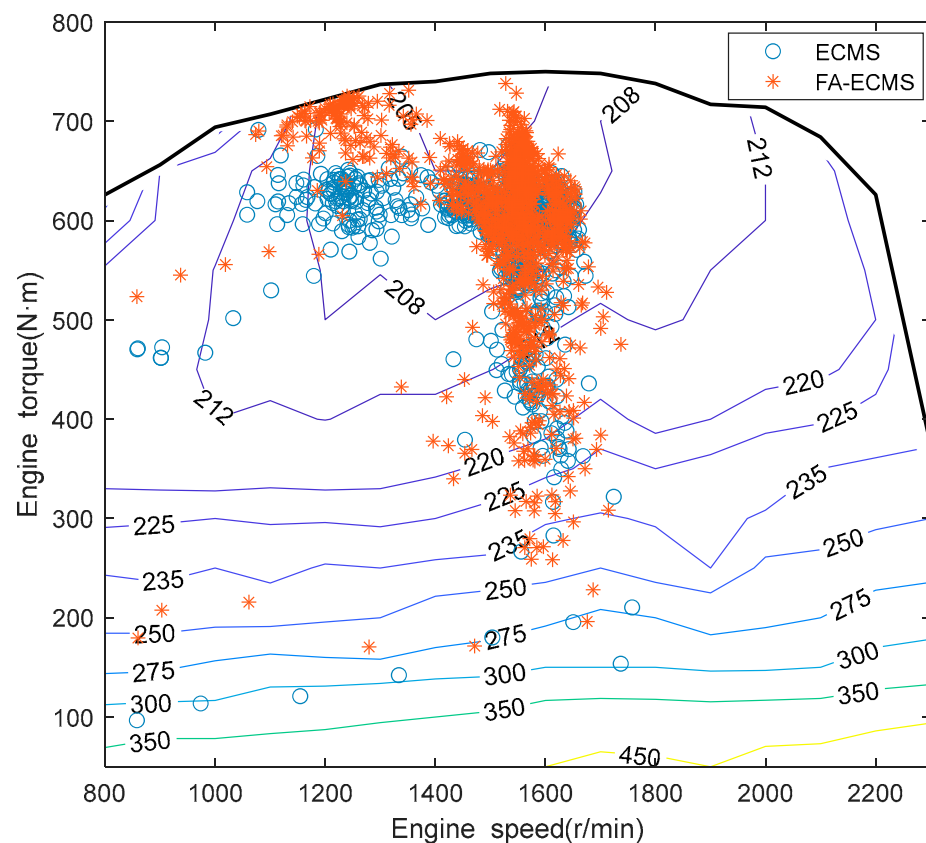


Figure 17. Comparison of engine operating point distribution under plowing cycle.

5.4. Analysis of the Road Transport Cycle

Figure 18 shows the simulation results of the hybrid tractor with ECMS strategy and FA-ECMS strategy under the modified EUDC cycle. The speed under different strategies is shown in Figure 18a,b. It can be seen that the actual speed of the tractor can track the target speed well under both ECMS and FA-ECMS, and the average speed deviation is very low, which can meet the simulation accuracy requirements. The distribution of engine and motor power is shown in Figure 18c,d. Combined with the change of SOC trajectory in Figure 18e, it can be seen that the results of the two strategies for engine and motor power distribution are consistent before 110 s of simulation, and the deviation of SOC trajectory becomes more obvious as the simulation advances. The maximum deviation of 5.57% exists at 200 s, and the SOC under ECMS strategy and FA-ECMS strategy at the end of the working cycle is 60.32% and 60.17%, respectively. Under FA-ECMS strategy, the equivalent factor is in a state of real-time dynamic adjustment. Overall, the FA-ECMS strategy takes more time to charge the motor compared to the ECMS strategy, which is more conducive to increasing the load on the engine, causing the operating point to migrate toward the efficient operating zone, thus reducing overall fuel consumption. The optimized FA-ECMS strategy has a fuel consumption of 1.13 L for one duty cycle, which is 5.04% fuel saving compared to the ECMS strategy, with a fuel consumption of 1.19 L. Figure 19 compares the distribution of engine operating points, which are more distributed in the efficient engine operating zone with the FA-ECMS strategy compared to the ECMS strategy.

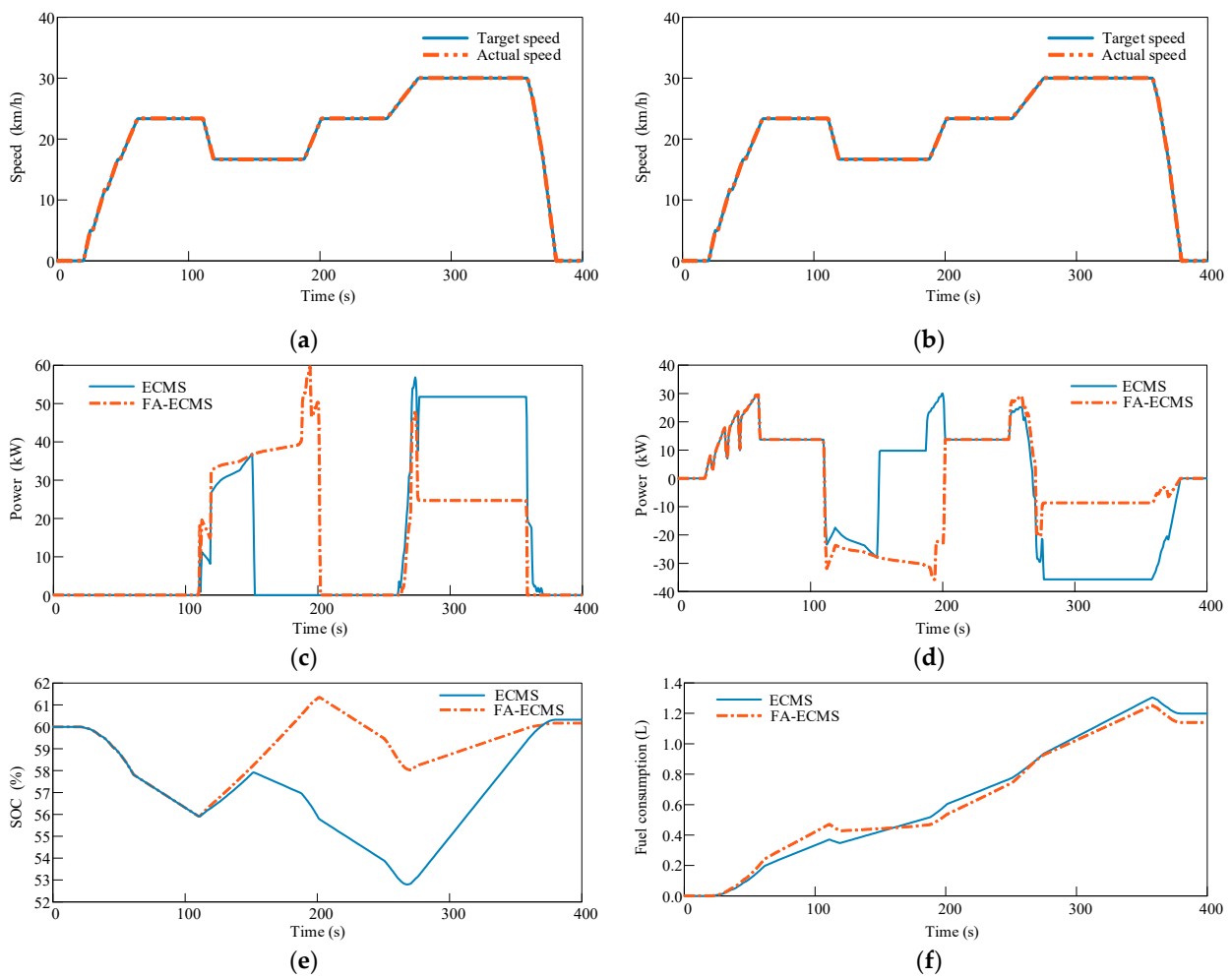


Figure 18. Results of road transport cycle: (a) speed following situation under ECMS; (b) speed following situation under FA-ECMS; (c) engine power comparison; (d) motor power comparison; (e) comparison of battery SOC trajectories; (f) comparison of fuel economy.

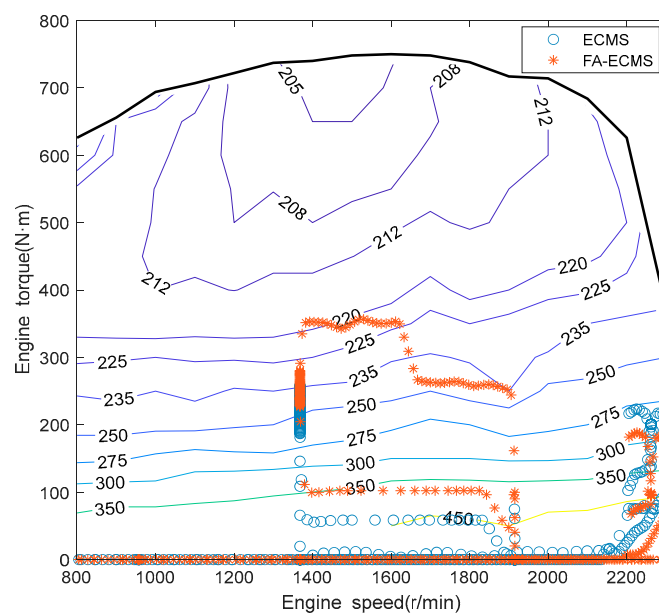


Figure 19. Comparison of engine operating point distribution under road transport cycle.

5.5. Comparative Analysis of Simulation Results

As shown in Tables 5 and 6, under the plowing cycle, the fuel consumption of the traditional ECMS strategy and the FA-ECMS strategy is 14.30 L and 13.34 L, respectively, while under the road transport cycle it is 1.19 L and 1.13 L, respectively. After the fuzzy adaptive adjustment of the equivalent factor, the fuel consumption of the tractor is reduced by 6.71% and 5.04%. Moreover, the engine operating points are distributed in the high efficiency interval. In terms of power maintenance, the battery SOC under the traditional ECMS strategy and the FA-ECMS strategy is 60.75% and 60.27%, respectively, under the plowing cycle, and 60.32% and 60.17%, respectively, under the transportation cycle. Under the FA-ECMS strategy, the battery power is closer to the target SOC after the working cycle, reflecting better power maintenance performance.

Table 5. Comparison of fuel consumption.

Cycles	Fuel Consumption under ECMS	Fuel Consumption under FA-ECMS	Fuel Saving Rate
Plowing	14.30 L	13.34 L	6.71%
Transport	1.19 L	1.13 L	5.04%

Table 6. Comparison of battery SOC.

Cycles	Initial SOC	Final SOC under ECMS	Final SOC under FA-ECMS
Plowing	60%	60.75%	60.27%
Transport	60%	60.32%	60.17%

6. Conclusions

This paper presents a powertrain configuration for a hybrid agricultural tractor equipped with a HMCVT by integrating hybrid technology with continuously variable transmission technology. The operating mode of the hybrid agricultural tractor was analyzed, and the transmission mode and speed ratio characteristics of the HMCVT were introduced. According to the characteristics of the designed hybrid tractor, a tractor working mode division strategy based on logic thresholds was developed to divide the tractor working mode. In terms of engine and motor power distribution of the hybrid tractor, a fuzzy adaptive equivalent fuel consumption minimization strategy was proposed. A fuzzy PI controller was introduced to dynamically adjust the fixed equivalent factor in the traditional ECMS. An adaptive model of the equivalent factor was established.

Two typical cycles, tractor plowing and road transport, were separately simulated. After the improvement of the energy management strategy, the tractor was able to achieve fuel savings in the plowing cycle and road transport cycle compared to the previous strategy, with more of the engine's operating points distributed in the efficient areas. In terms of SOC maintenance, the SOC values of the battery at the end of the cycles were closer to the initial target value after the improvement of the strategy. The study may provide a reference solution for energy savings and consumption reduction in hybrid agricultural tractors.

In future research, we will conduct experiments that consider practical influences, such as the effect of temperature on the efficiency of batteries and hydraulic components, to further validate the reliability of the control strategy in a real-world application environment.

7. Patents

The powertrain system reported in this manuscript has been authorized in China (Authorization No. CN109723789B, Patent No. CN201910041132.1).

Author Contributions: Conceptualization, Z.Z. and L.Z.; methodology, Z.Z.; software, L.Z.; validation, L.C., R.Z. and Y.C.; formal analysis, L.C.; investigation, R.Z.; resources, Y.C. and L.C.; data curation, Z.Z. and L.Z.; writing—original draft preparation, Z.Z. and L.Z.; writing—review and editing, Z.Z. and L.Z.; visualization, Z.Z. and L.Z.; supervision, Y.C.; project administration, L.C., R.Z. and Y.C.; funding acquisition, Z.Z., Y.C., L.C. and R.Z. All authors have read and agreed to the published version of the manuscript.

Funding: This research was funded by the National Natural Science Foundation of China (52272435, 52225212, U20A20333, U20A20331, 51875255), Key Research and Development Program of Jiangsu Province (BE2020083-3, BE2019010-2), Jiangsu Province and Education Ministry Co-sponsored Synergistic Innovation Center of Modern Agricultural Equipment (XTCX2020).

Institutional Review Board Statement: Not applicable.

Data Availability Statement: The data that support the findings of this study are available from the corresponding author at caicaixiao0304@126.com upon reasonable request.

Conflicts of Interest: The authors declared no potential conflict of interest.

References

1. Data Query System of Ministry of Agriculture and Rural Affairs of the People's Republic of China. Available online: <http://zdsccx.moa.gov.cn:8080/nyb/pc/search.jsp> (accessed on 15 July 2022).
2. Guo, S. The present situation and consideration of agricultural mechanization development in China. *South. Agric. Mach.* **2022**, *53*, 79–82.
3. Liu, M.; Lei, S.; Zhao, J. Development process and research status of electric tractor. *Trans. Chin. Soc. Agric. Mach.* **2022**, *12*, 1547.
4. Xie, B.; Wu, Z.; Mao, E. Development and prospect of key technologies on agricultural tractor. *Trans. Chin. Soc. Agric. Mach.* **2018**, *49*, 1–17.
5. Malik, A.; Kohli, S. Electric tractors: Survey of challenges and opportunities in India. *Mater. Today Proc.* **2020**, *28*, 2318–2324. [[CrossRef](#)]
6. Dalboni, M.; Santarelli, P.; Patroncini, P.; Soldati, A.; Concari, C.; Lusignani, D. Electrification of a Compact Agricultural Tractor: A Successful Case Study. In Proceedings of the 2019 IEEE Transportation Electrification Conference and Expo (ITEC), Detroit, MI, USA, 19–21 June 2019; IEEE: Piscataway, NJ, USA; pp. 1–6.
7. Mocera, F.; Martini, V. Numerical Performance Investigation of a Hybrid eCVT Specialized Agricultural Tractor. *Appl. Sci.* **2022**, *12*, 2438. [[CrossRef](#)]
8. Rossi, C.; Pontara, D.; Falcomer, C.; Bertoldi, M.; Mandrioli, R. A Hybrid–Electric Driveline for Agricultural Tractors Based on an e-CVT Power-Split Transmission. *Energies* **2021**, *14*, 6912. [[CrossRef](#)]
9. Mocera, F.; Somà, A. Analysis of a Parallel Hybrid Electric Tractor for Agricultural Applications. *Energies* **2020**, *13*, 3055. [[CrossRef](#)]
10. Wu, Z.; Xie, B.; Chi, R.; Ren, Z.; Du, Y.; Li, Z. Driving torque management model for electric tractor in field cruise condition. *Trans. CSAE* **2019**, *35*, 88–98.
11. Jia, C.; Qiao, W.; Qu, L. Numerical Methods for Optimal Control of Hybrid Electric Agricultural Tractors. In Proceedings of the 2019 IEEE Transportation Electrification Conference and Expo (ITEC), Detroit, MI, USA, 19–21 June 2019; IEEE: Piscataway, NJ, USA; pp. 1–6.
12. Rodriguez, R.; Trovão, J.P.F.; Solano, J. Fuzzy logic-model predictive control energy management strategy for a dual-mode locomotive. *Energy Convers. Manag.* **2022**, *253*, 115111. [[CrossRef](#)]
13. Tang, X.; Yang, K.; Wang, H.; Yu, W.; Yang, X.; Liu, T.; Li, J. Driving Environment Uncertainty-Aware Motion Planning for Autonomous Vehicles. *Chin. J. Mech. Eng.* **2022**, *35*, 120. [[CrossRef](#)]
14. Yang, Y.; Xu, Y.; Zhang, H.; Yang, F.; Ren, J.; Wang, X.; Jin, P.; Huang, D. Research on the energy management strategy of extended range electric vehicles based on a hybrid energy storage system. *Energy Rep.* **2022**, *8*, 6602–6623. [[CrossRef](#)]
15. Mocera, F. A Model-Based Design Approach for a Parallel Hybrid Electric Tractor Energy Management Strategy Using Hardware in the Loop Technique. *Vehicles* **2020**, *3*, 1. [[CrossRef](#)]
16. Tebaldi, D.; Zanasi, R. Modeling Control and Simulation of a Parallel Hybrid Agricultural Tractor. In Proceedings of the 2021 29th Mediterranean Conference on Control and Automation (MED), PUGLIA, Italy, 22–25 June 2021; IEEE: Piscataway, NJ, USA; pp. 317–323.
17. Scolaro, E.; Alberti, L.; Barater, D. Electric Drives for Hybrid Electric Agricultural Tractors. In Proceedings of the 2021 IEEE Workshop on Electrical Machines Design, Control and Diagnosis (WEMDCD), Modena, Italy, 8–9 April 2021; IEEE: Piscataway, NJ, USA; pp. 331–336.
18. Xu, L.; Liu, E.; Liu, M. Energy management strategy of fuel cell and storage battery hybrid electric tractor. *J. Henan Univ. Sci. Technol. Nat. Sci.* **2019**, *40*, 80–86.
19. Jia, C.; Qiao, W.; Qu, L. Modeling and Control of Hybrid Electric Vehicles: A Case Study for Agricultural Tractors. In Proceedings of the 2018 IEEE Vehicle Power and Propulsion Conference (VPPC), Chicago, IL, USA, 27–30 August 2018; IEEE: Piscataway, NJ, USA; pp. 1–6.

20. Li, Q.; Zou, X.; Pu, Y.; Chen, W. A real-time energy management method for electric-hydrogen hybrid energy storage microgrid based on DP-MPC. *CSEE J. Power Energy Syst.* **2020**, 1–13. [[CrossRef](#)]
21. Li, T.; Xie, B.; Wang, D.; Zhang, S.; Wu, L. Real-time adaptive energy management strategy for dual-motor-driven electric tractors. *Trans. Chin. Soc. Agric. Mach.* **2020**, 51, 530–543.
22. Li, Y.; Liu, L.; Jin, T.; Yuan, K.; Chen, Y. Energy control strategy of electric tractor power supply based on dynamic programming. *Trans. Chin. Soc. Agric. Mach.* **2020**, 51, 403–410.
23. Tian, X.; Cai, Y.; Sun, X.; Zhu, Z.; Xu, Y. An adaptive ECMS with driving style recognition for energy optimization of parallel hybrid electric buses. *Energy* **2019**, 189, 116151. [[CrossRef](#)]
24. Xie, P.; Tan, S.; Guerrero, J.M.; Vasquez, J.C. MPC-informed ECMS based real-time power management strategy for hybrid electric ship. *Energy Rep.* **2021**, 7, 126–133. [[CrossRef](#)]
25. Yao, M.; Zhu, B.; Zhang, N. Adaptive real-time optimal control for energy management strategy of extended range electric vehicle. *Energy Convers. Manag.* **2021**, 234, 113874. [[CrossRef](#)]
26. Wang, S.; Huang, X.; Lopez, J.M.; Xu, X.; Dong, P. Fuzzy Adaptive-Equivalent Consumption Minimization Strategy for a Parallel Hybrid Electric Vehicle. *IEEE Access* **2019**, 7, 133290–133303. [[CrossRef](#)]
27. Geng, W.; Lou, D.; Zhang, T. Multi-objective energy management strategy for hybrid electric vehicle based on particle swarm optimization. *J. Tongji Univ. Nat. Sci.* **2020**, 48, 1030–1039.
28. Onori, S.; Serrao, L.; Rizzoni, G. *Hybrid Electric Vehicles: Energy Management Strategies*; Springer: London, UK, 2016.
29. Siddique, M.A.A.; Kim, Y.-J.; Baek, S.-M.; Baek, S.-Y.; Han, T.-H.; Kim, W.-S.; Kim, Y.-S.; Lim, R.-G.; Choi, Y. Development of the Reliability Assessment Process of the Hydraulic Pump for a 78 kW Tractor during Major Agricultural Operations. *Agriculture* **2022**, 12, 1609. [[CrossRef](#)]
30. EPA Nonregulatory Nonroad Duty Cycles. Available online: <https://www.epa.gov/moves/epa-nonregulatory-nonroad-duty-cycles> (accessed on 15 March 2022).